

Effective Date: 11/23/2022

Expiration Date: 11/23/2027

XRISM/ Resolve
CMO
11/23/2022
RELEASED

INSTRUMENT CALIBRATION REPORT

RESOLVE ANTICOINCIDENCE DETECTOR GAIN

RESOLVE-SCI-RPT-0055

REVISION (A)

XRISM-RESOLVE-CALDB-GAINANT-215

X-ray Imaging and Spectroscopy Mission (XRISM) Project

NASA/GSFC Code 461



Goddard Space Flight Center
Greenbelt, Maryland

National Aeronautics and
Space Administration

Check <https://ipdtdms.gsfc.nasa.gov>
to verify that this is the correct version prior to use

RESOLVE ANTICOINCIDENCE DETECTOR GAIN

Signature/Approval Page

Prepared by: Renata Cumbee, Megan Eckart, Caroline Kilbourne, Scott Porter, Maurice Leutenegger, and the Resolve Instrument Team

Reviewers/Approvers:

Megan Eckart
Maurice Leutenegger
Renata Cumbee
Matthew Holland
Caroline Kilbourne
Michael Lowenstein
Scott Porter
Tahir Yaqoob

Approved by:

Megan Eckart

*** Electronic signatures are available on-line at: <https://ipdtdms.gsfc.nasa.gov>***

Preface

This document is an XRISM Project signature-controlled document. Changes to this document require prior approval of the applicable Product Design Lead (PDL) or designee. Proposed changes shall be submitted in the Technical Data Management System (TDMS) via a Signature Control Request (SCoRe) along with supportive material justifying the proposed change. Changes to this document will be made by complete revision.

All of the requirements in this document assume the use of the word "shall" unless otherwise stated.

Questions or comments concerning this document should be addressed to:
XRISM Configuration Management Office
Mail Stop: 461
Goddard Space Flight Center
Greenbelt, Maryland 20771

NOTE to editors: The document name will be XRISM-CAL-RPT-XXXX, where XXXX is assigned by the TDMS system. The document will be cross-referenced in TDMS to the filename in the format XRISM-XXX-CALDB-FILEDESC-NN where XXX is the instrument or component (e.g. RESOLVE), FILEDESC refers to a specific calibration report (e.g., rmfparams) and NN the corresponding number assigned to that report by the SDC. For example the calibration report addressing the Resolve LSF calibration may be assigned XRISM-RESOLVE-CALDB-RMFPARAMS-01, that addressing the Resolve gain calibration XRISM-RESOLVE-GAINPIX-CALDB-02, etc. (where the numbers are to be provided by the SDC).

These documents are updated as needed, e.g. when the relevant CALDB files, or the relevant calibration data analysis, is revised. The document version will be assigned by the TDMS system. The tracking tool should be used to record changes.

This document must include the CalDB file name, an explanation of how the data were collected and the analysis conducted and, if using standard Ftools, the software version number. All revisions are consolidated into the same document to maintain a full record of all changes.

Table of Contents

1	Introduction.....	1
1.1	Purpose.....	1
1.2	Scientific Impact.....	1
2	First Delivery – 20190522.....	1
2.1	Data Description	2
2.2	Data Analysis	3
2.3	Results.....	7
2.4	Final remarks	7
3	Second Delivery – 20220210	7
3.1	Data Description	7
3.2	Data Analysis	9
3.3	Results.....	14
3.4	Final remarks	14
4	References.....	14

1 Introduction

1.1 Purpose

A fraction of cosmic rays that traverse the Resolve calorimeter pixels will leave behind energy comparable to photons in the Resolve bandpass. An anti-coincidence detector (“anti-co”) provides an independent monitor of the particle environment and serves to reject cosmic ray events. The coincidence rejection (i.e., removal of cosmic-ray events) is performed on ground. The Resolve anti-co system employs a low voltage silicon ionization detector placed directly behind the main array. Calorimeter events that arise from ionizing particles can thus be vetoed as they will also trigger a pulse in the anti-co detector. The anti-co signals are amplified and digitized by the XBOX, and the digital data is then sent to the Pulse Shape Processor (PSP) for pulse detection and processing. The XBOX has two sides (XBOX-A and XBOX-B), which each handle input from half of the detector channels and one of the two anti-co channels. The two anti-co channels are completely redundant. Each side is independent such that if one side fails half of the detector channels and one of the anti-co channels remain active. Each anti-co event contains an arrival time, duration, and pulse height. With these three parameters, the event reduction software can flag calorimeter events based on relative timing to an anti-co pulse that meets the minimum pulse height amplitude (PHA) and duration criteria for a cosmic ray event. The anti-co is described in more detail in references [1] and [2].

This document describes the CALDB gain file for the Resolve anti-coincidence detector and is based on the *Hitomi* SXS CALDB report [3].

1.2 Scientific Impact

The anti-co gain is used to convert anti-co PHA (in ADC units) to PI (pulse height invariant in energy in keV). The anti-co events may be used to flag cosmic ray events in the pipeline task `rs1flagpix`.

2 First Delivery – 20190522

Filename	Valid date	Delivery date	Comments
xa_rsl_gainant_20190101v001.fits	2018-10-12	2019-05-22	Original ASCII file: AnticoGain_20190522_v0c.txt

2.1 Data Description

The calibration of the anti-co gain was performed using the Resolve flight model detector system in a laboratory dewar on October 12, 2018 at GSFC using the engineering model XBOX. We used a Rotating Target X-ray Source (RTS) to provide x-ray lines at known energies.

The RTS consists of a bright x-ray continuum source (TruFocus model 5110 with tungsten target) that illuminates single crystal targets mounted on a rotating wheel. Fluorescence from the targets provides x-ray line emission directed to the instrument aperture. For the case of the anti-co gain measurement we used the RTS in rotating mode to provide a flux of x-rays at various dwell times, shown in Table 1, for a total of 26.5 hours. The x-ray source settings were HV=30 kV and $I_{\text{emission}} = 3 \mu\text{A}$.

Slot	Target	Dwell Time (s)
0	Ag	150
1	KBr	30
2	Cu	10
3	GaAs	40
4	Mo	38
5	Y	23
6	Mn	10
7	TiO ₂	27

Table 1: The RTS targets during anti-co gain measurements at GSFC on 10/12/18, and their dwell times.

The data were acquired using the engineering model Pulse Shape Processor (PSP). The PSP calculates the pulse height amplitude (PHA) of each anti-co event by subtracting the anti-co pedestal from the raw pulse height (the maximum ADC sample for each triggered event, ADC_SAMPLE_MAX). The anti-co pedestal (ADC_SAMPLE_PEDESTAL) is a commandable value that was determined to 'zero' the anti-co PHA so that histograms of anti-co baseline events are centered at the origin. Table 2 provides a summary of relevant PSP parameters.

Anti-co Channel ID	Anti-co Pedestal [ADC units]	Anti-co Threshold [ADC units]
0 (PSP side A)	-6531	25
2 (PSP side B)	-6530	25
PSP UAPP_VER: 0x141118		

Table 2: Relevant PSP parameters during anti-co gain calibration measurement. There is a single anticoincidence detector, but, for redundancy, it is read out using two separate readout chains.

The instrument was in a nominal operating state with a detector temperature of 50mK and an anti-co bias of 6V for each channel. The Resolve data were recorded into an Igor Pro experiment, filename = 18-10-12.20.38.55Z.pxp using the XRSGSE software suite version 11.1.4, with corresponding raw files 2018_1012_1641_46_side_a.xbox_raw and 2018_1012_1641_46_side_b.xbox_raw.

2.2 Data Analysis

The anticoincidence detector is linear over its operating range of ~1 keV – 6 MeV. We parameterize the anti-co gain as follows:

$$E \text{ [keV]} = \text{coef0} + \text{coef1} * \text{PHA} + \text{coef2} * \text{PHA}^2 + \text{coef3} * \text{PHA}^3. \quad \text{Eq. (1)}$$

The anti-co gain is primarily described by the linear coefficient (coef1). The offset coefficient (coef0) is included to correct any sub-ADC-sample shift in the zero-point, which is likely since the pedestal is limited to an integral number of ADC units. We expect that the quadratic and cubic terms (coef2 and coef3) will always be zero, but include them for flexibility.

Figure 1 presents the anti-co spectrum for Channel 0 (PSP side A) and Channel 2 (PSP side B). To derive the anti-co gain we require a precise measure of the centroid of the center of mass $K\alpha$ line complex for Br, Y, Mo, and Ag. We performed a Gaussian fit to each $K\alpha$ line as well as the anti-co baseline events to determine the sub-ADC-unit offset parameter. The fit results are presented in Table 3. The gain parameters are determined using these parameters and assuming linearity (coef2=coef3=0). The data show each anti-co channel has a scaling of ~0.43 keV per ADC unit. Because the Ag $K\alpha$ line is blended with the Ag $K\beta$ line, we performed a two-Gaussian fit of the Ag $K\alpha$ and $K\beta$ region. We found that the resulting fit was skewed by the counts at lower energy, and additionally performed a four-gaussian fit, as shown in Figure 2. It was found that the energy derived from the fit of the Ag $K\alpha$ line is skewed by blending with the $K\beta$ line by ~0.048 ADC units for Channel 2, but no difference is observed for Channel 0. This difference has a minor effect on the fitting parameters coef0 and coef1, and will be explored in more detail in the next release of this report.

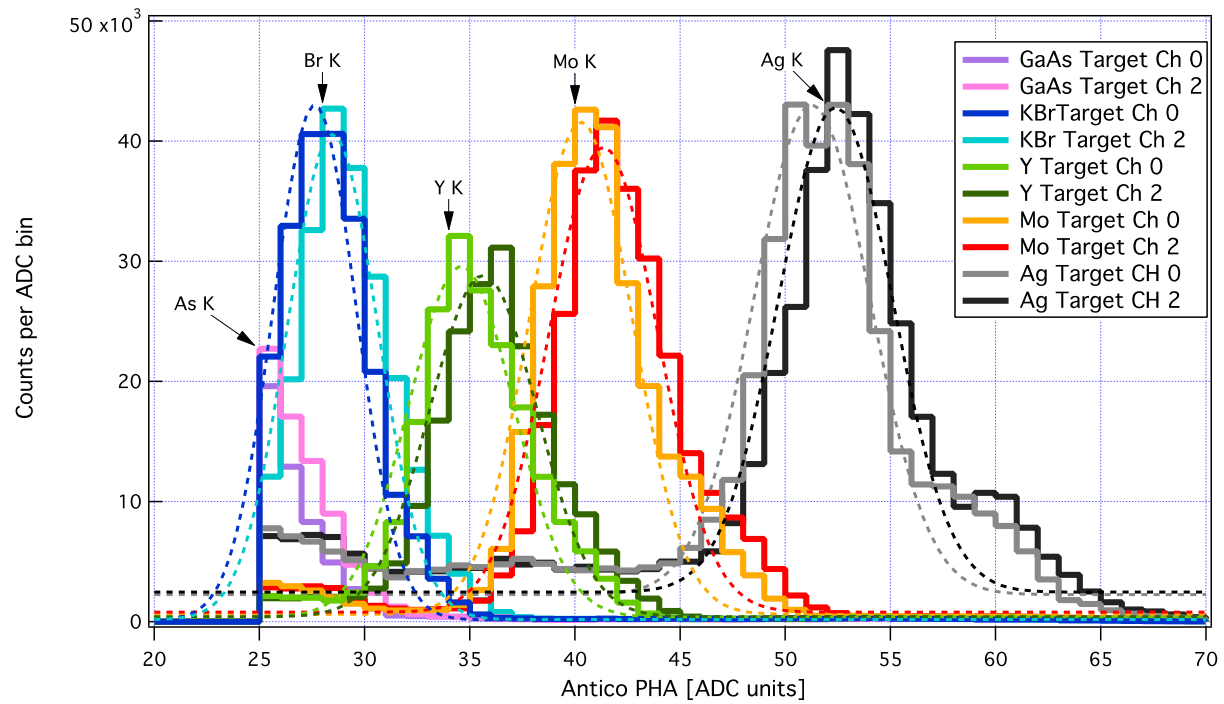


Figure 1: Anti-co channel 0 and channel 2 spectra (solid curves) and corresponding Gaussian fits (dashed curves).

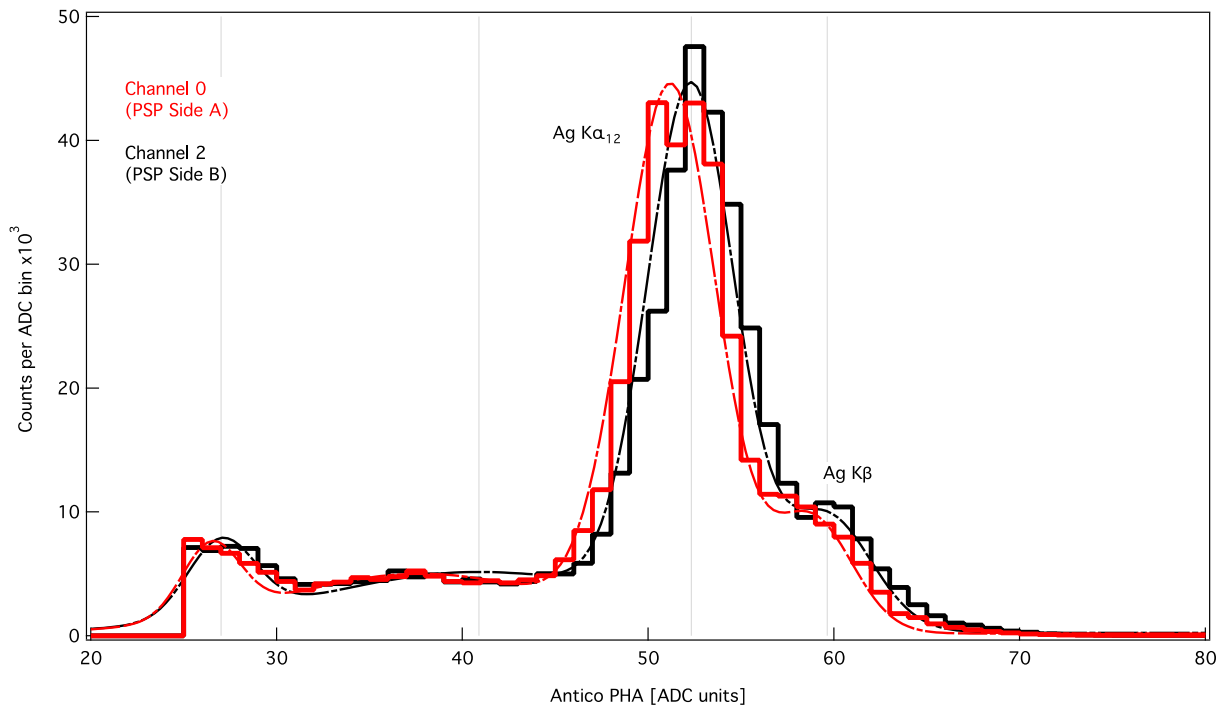


Figure 2: Ag $K\alpha$ and $K\beta$ Ch 0 (red) and Ch 2 (black) spectra and corresponding fits (dotted-dashed lines).

Line ID	PH Ch 0 (ADC units)	PH Ch 2 (ADC units)	Energy (keV)
	-0.12	0.64	0
Br $K\alpha$	27.5	28.41	11.9087
Y $K\alpha$	34.48	35.57	14.9332
Mo $K\alpha$	40.05	41.12	17.4443
Ag $K\alpha$	51.21	52.28	22.1054

Table 3: Fit results for line centroids for Ch 0 and Ch 2 in ADC units, and the corresponding center of mass line energies.

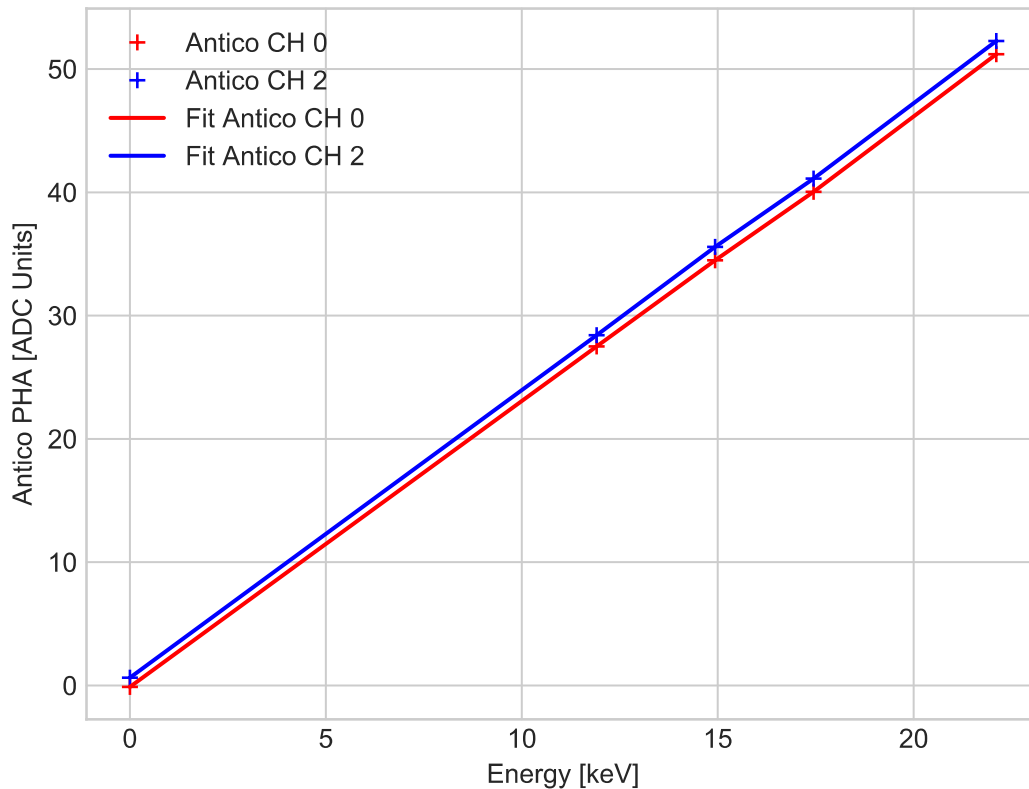


Figure 3: Calibration of the energy scale using a linear fit to the calibration data (Table 3).

Note that the anti-co lines show an asymmetric distribution, with a tail towards low energies, due to an arrival-time–PHA dependence. This asymmetry is not as apparent at low energies (e.g., in the bandpass measured here compared to the 6 MeV operating bandpass of the anti-co), but becomes more pronounced at higher energies. Thus a simple PHA–energy gain conversion becomes less-well-defined at higher energies; however, the only requirement on the knowledge of the anti-co energy scale is to provide knowledge of the energy and resolution near the threshold, which is typically set at ~ 10 keV. Having information about the rest of the spectrum is expected to be an interesting diagnostic, but there is no requirement on it.

2.3 Results

The CALDB file contains the polynomial coefficients, as defined in Eq. 1, for each anti-co channel. The results are displayed in Table 4.

Anti-co Channel ID	coef0 [keV]	coef1 [keV/ADC]	coef2 [keV/ADC ²]	coef3 [keV/ADC ³]
0 (PSP Side A)	0.0594	0.4316	0.0	0.0
2 (PSP Side B)	-0.2711	0.4287	0.0	0.0

Table 4 Resolve anti-co gain coefficients.

The uncertainty on the offset (coef0) values are ~ 0.13 keV; the uncertainty on the scaling terms (coef1) are ~ 0.009 keV/ADC. Thus, within the uncertainty, the A-side and B-side gains are the same.

2.4 Final remarks

This is the first release of this CALDB file based on ground measurements using the Resolve detector system in a laboratory dewar and an engineering model XBOX. The CALDB file and this document will be updated once data is taken using the flight model dewar and XBOX.

3 Second Delivery – 20220210

Filename	Valid date	Delivery date	Comments
xa_rsl_gainant_20190101v002.fits	2019-09-17	2022-02-10	Original ASCII file: AnticoGain_20220210_v0a.txt

3.1 Data Description

The calibration of the anti-co gain was performed during Resolve instrument-level test (TC5) at TKSC on February 10, 2022 using the Resolve flight model (FM) detector system, dewar, and XBOX. The 16-slot RTS [4], which uses the Newton Scientific M47 X-ray tube with a W target, was used to illuminate 4 of the 16 crystal targets mounted on the rotating target wheel. Fluorescence from the targets provides x-ray line emission directed to the instrument aperture.

For this measurement, the 16-slot RTS was used in rotating mode to provide a flux of x-rays at various dwell times, shown in Table 1, for a total of 2.5 hours. The x-ray source settings were HV=50 kV and $I_{\text{emission}} = 5 \mu\text{A}$.

Slot	Target	Dwell Time (s)
0	V	-
1	Ni	-
2	Cu	-
3	Fe	-
4	Zn	-
5	Sc	-
6	Ti	-
7	Y	12
8	Mn	-
9	Cr	-
10	Mo	10
11	KBr	-
12	BaF2	52
13	Co	-
14	Ge	-
15	Ag	14

Table 5: The RTS targets during anti-co gain measurements at TKSC on 02/10/22, and their dwell times.

Similar to the first delivery in Section 2, the data were acquired using the flight model Pulse Shape Processor (PSP). The PSP calculates the pulse height amplitude (PHA) of each anti-co event by subtracting the anti-co pedestal from the raw pulse height (the maximum ADC sample for each triggered event, ADC_SAMPLE_MAX). The anti-co pedestal (ADC_SAMPLE_PEDESTAL) is a commandable value that was determined to ‘zero’ the anti-co PHA so that histograms of anti-co baseline events are centered at the origin. The anti-co pedestal was modified from the last delivery due to the change from the EM XBOX to the FM XBOX; this delivery’s validity date corresponds to the first use of the FM XBOX with the updated pedestals. Table 6 provides a summary of relevant PSP parameters.

Anti-co Channel ID	Anti-co Pedestal [ADC units]	Anti-co Threshold [ADC units]
0 (PSP side A)	-6616	25
2 (PSP side B)	-6615	25
PSP UAPP VER: 0x150615		

Table 6: Relevant PSP parameters during anti-co gain calibration measurement. There is a single anticoincidence detector, but, for redundancy, it is read out using two separate readout chains.

The instrument was in a nominal operating state with a detector temperature of 50mK and an anti-co bias of 6V for each channel. The Resolve data were recorded into an Igor Pro experiment, filename = TC5_helium_22-02-10.01.01.21Z.pxp using the XRSGSE

software suite version 12.1.6, with corresponding raw files
 2022_0210_1106_17_side_a.xbox_raw
 and 2022_0210_1106_17_side_b.xbox_raw.

3.2 Data Analysis

As described in Section 2.2, the anticoincidence detector is linear over its operating range of ~ 1 keV – 6 MeV. As described in Eq. 1, the anti-co gain is primarily described by the linear coefficient (coef1) with the offset coefficient (coef0) correcting any sub-ADC-sample shift in the zero-point.

Figure 4 presents the anti-co spectrum for Channel 0 (PSP side A) and Channel 2 (PSP side B) while Figure 5 presents the same spectra with the gain scale incorporated. To derive the anti-co gain we require a precise measure of the centroid of the center of mass $K\alpha$ line complex for Y, Mo, Ag, and Ba. We performed a Gaussian fit to each $K\alpha$ line as well as the anti-co baseline events to determine the sub-ADC-unit offset parameter. The fit results are presented in Table 7. The gain parameters are then determined using these parameters and assuming linearity (coef2=coef3=0). The data in Table 8 show that each anti-co channel has a scaling of ~ 0.43 keV per ADC unit, similar to the values presented in the first delivery in Section 2.

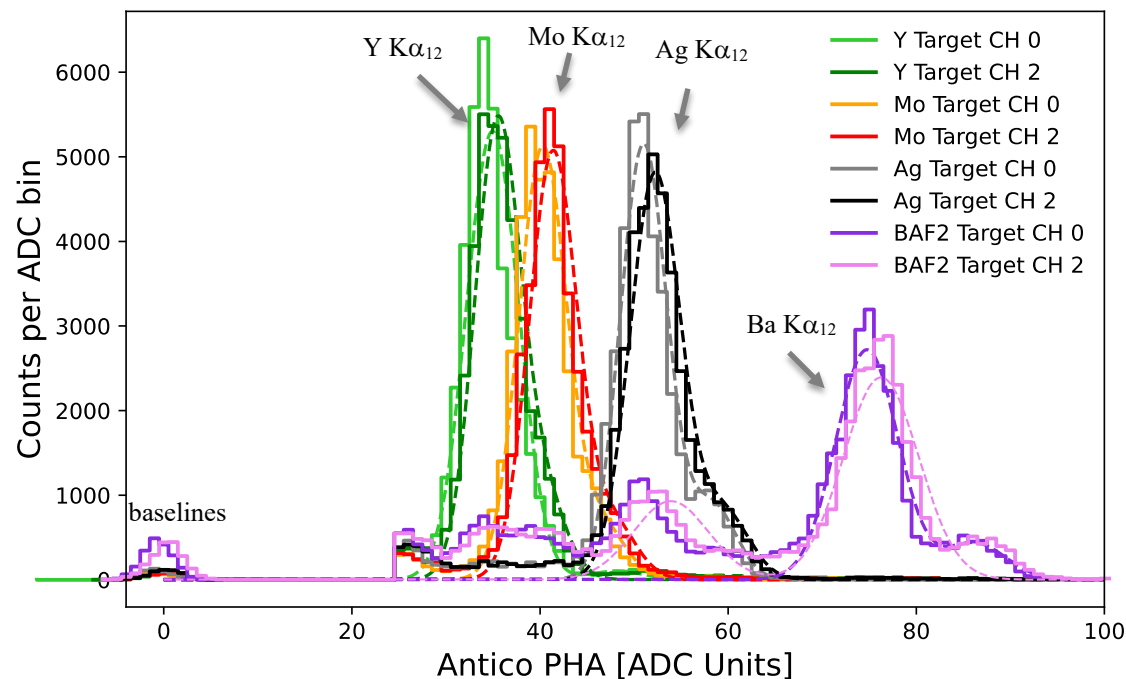


Figure 4: Anti-co channel 0 and channel 2 spectra (solid curves) and corresponding Gaussian fits (dashed curves).

Line ID	PH Ch 0 (ADC units)	PH Ch 2 (ADC units)	Energy (keV)
	-0.44	0.64	0
Y $K\alpha$	34.95	35.45	14.9332
Mo $K\alpha$	40.28	41.83	17.4443
Ag $K\alpha$	51.11	52.38	22.1054
Ba $K\alpha$	74.87	76.15	32.1936

Table 7: Fit results for line centroids for Ch 0 and Ch 2 in ADC units, and the corresponding center of mass line energies.

In Section 2.2, it was shown that a four-gaussian fit was needed to constrain the center of the Ag $K\alpha$ line due to blending with the $K\beta$ line as well as counts at lower energies. Here, we performed a similar analysis by performing a two-gaussian fit to include both the $K\alpha$ and $K\beta$ lines for Ag and Ba, as well as an additional four-gaussian fit for Ag and a five-gaussian fit for Ba to include any shift in derived energy due to lower energy counts. In performing a two gaussian fit, we determined that energy derived for the Ag $K\alpha$ line was skewed by the $K\beta$ line by ~ 0.1 ADC units for both Ch 0 and Ch 2. That two-gaussian derived energy was only skewed by ~ 0.08 ADC units when using a four-gaussian fit to include the lower energy counts. For BaF2, we found that the Ba $K\alpha$ line was also skewed by the $K\beta$ line by ~ 0.1 ADC units, but that energy was only skewed by ~ 0.03 ADC units by including a total of five gaussians to cover the lower energy counts, as shown in Figure 6.

The linear fit to the energies derived by these gaussian fits is shown in Figure 7. The differences in these derived energies only had a minor effect on the fitting parameters coef0 and coef1 . The difference in the linear fit for including single-gaussian fits (worse fit) and four and five-gaussian fits (best fit) for Ag and Ba was 0.0004 keV for coef0 , and $4. \times 10^{-5}$ keV/ADC for coef1 .

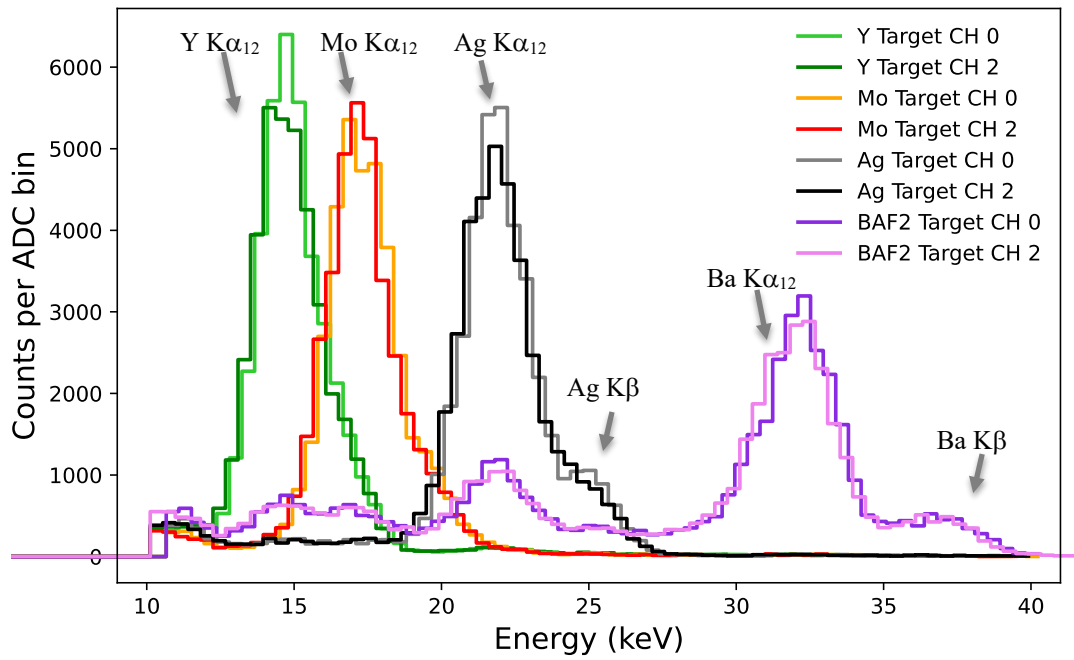


Figure 5: Anti-co channel 0 and channel 2 spectra with appropriate gain scale (Figure 7) included.

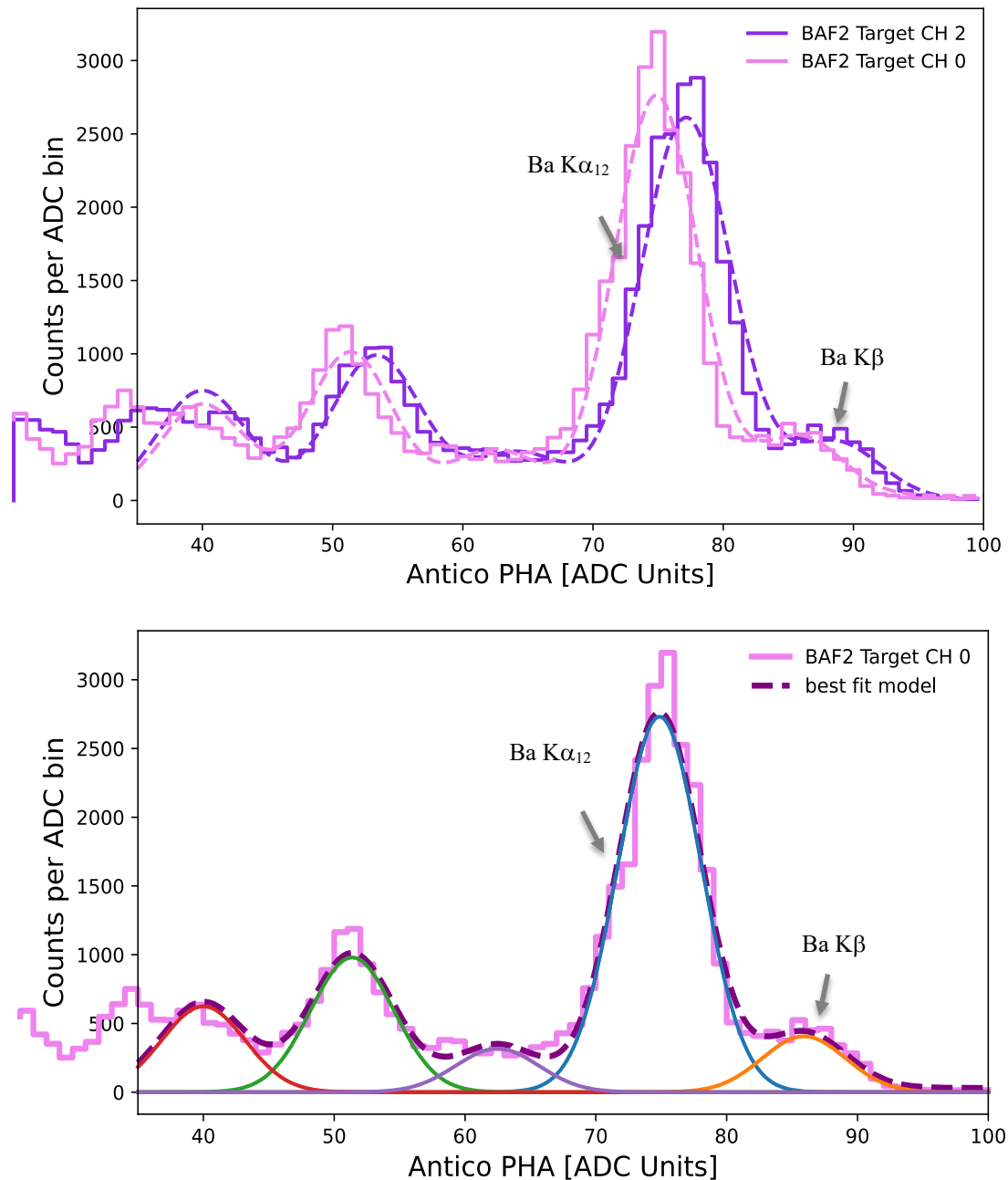


Figure 6: (Top) Ba K α and K β Ch 0 (magenta) and Ch 2 (violet) spectra and corresponding fits (dashed lines). (Bottom): A five-gaussian fit was performed to better constrain the Ba K α centroid, including any contribution from the K β line and any lower energy counts (shown for CH 0).

Note that the anti-co lines still show an asymmetric distribution, with a tail towards low energies,

due to an arrival-time–PHA dependence. This asymmetry is not as apparent at low energies (e.g., in the bandpass measured here compared to the 6 MeV operating bandpass of the anti-co) but becomes more pronounced at higher energies. Thus a simple PHA–energy gain conversion becomes less-well-defined at higher energies; however, the only requirement on the knowledge of the anti-co energy scale is to provide knowledge of the energy and resolution near the threshold, which is typically set at ~ 10 keV. Having information about the rest of the spectrum is expected to be an interesting diagnostic, but there is no requirement on it.

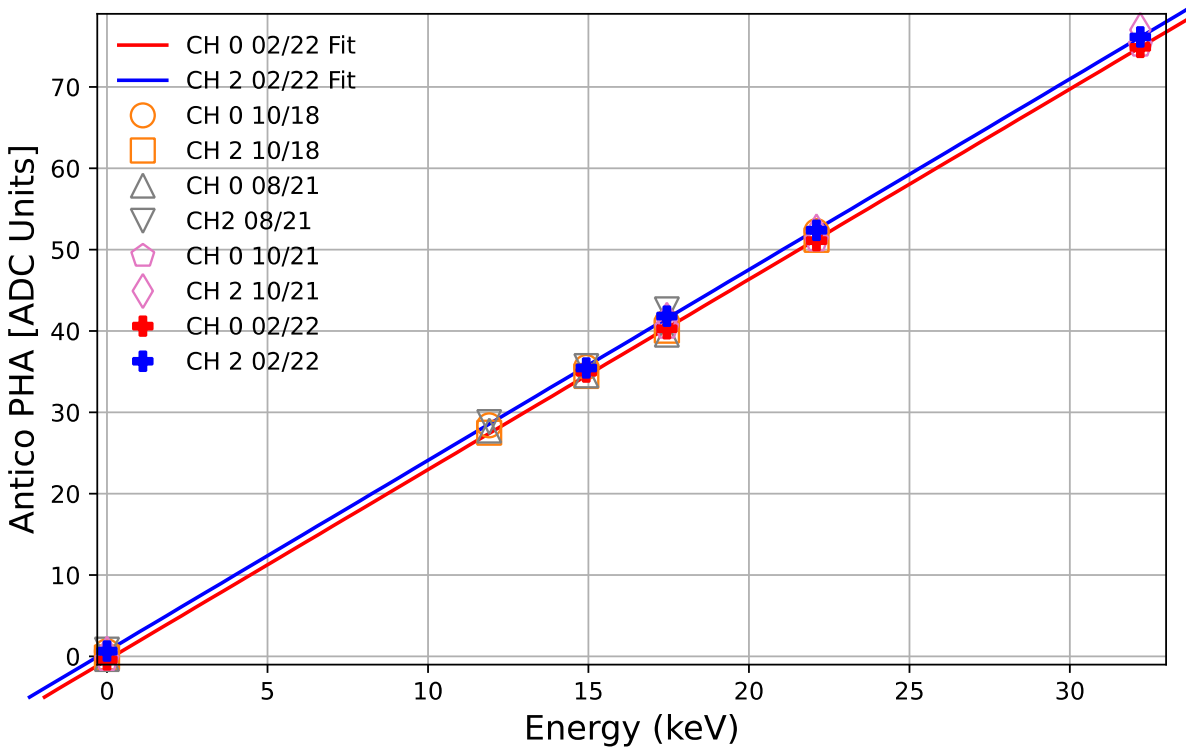


Figure 7: Calibration of the energy scale using a linear fit to the calibration data (Table 3). In addition to data points from this delivery (pluses), data from previous measurements (from 10/18 (the first delivery), 08/21, and 10/21) show agreement with the current fit.

3.3 Results

The CALDB file contains the polynomial coefficients, as defined in Eq. 1, for each anti-co channel. The results are displayed in Table 8.

Anti-co Channel ID	coef0 [keV]	coef1 [keV/ADC]	coef2 [keV/ADC ²]	coef3 [keV/ADC ³]
0 (PSP Side A)	0.1874+/-0.061	0.4274 +/- 0.006	0.0	0.0
2 (PSP Side B)	-0.2772+/-0.022	0.4265+/- 0.008	0.0	0.0

Table 8 Resolve anti-co gain coefficients.

The uncertainty on the offset (coef0) values are ~ 0.06 keV; the uncertainty on the scaling terms (coef1) are ~ 0.007 keV/ADC. As a comparison, a similar analysis was performed for previous anti-co measurements in which some EM hardware (XBOX, dewar, etc) was in use as shown in Figure 7. The coefficients determined from those measurements agree within the uncertainties reported in Table 8.

3.4 Final remarks

This is the final pre-flight release of this CALDB file based on ground measurements using the flight model Resolve detector system, dewar and XBOX.

4 References

- [1] C. A. Kilbourne et al., "Design, implementation, and performance of the Astro-H SXS calorimeter array and anticoincidence detector," JATIS, 4(1), 011214 (23 February 2018).
- [2] C. A. Kilbourne et al., "In-flight calibration of Hitomi soft x-ray spectrometer (1) background," Publ. Astron. Soc. Jpn. (2018).
- [3] M. Eckart, et al., "Instrument Calibration Report SXS Anticoincidence Detector Gain," asth_sxs_caldb_gainant_v20160310 (2016).
- [4] Resolve-sci-proc-0063_RevC: R. Cumbee et al., "Rotating Target Source (RTS) Operating Procedure"